arXiv:1405.4685v3 [cond-mat.mtrl-sci] 2 Apr 2015

Low-Dimensional Transport and Large Thermoelectric Power Factors in Bulk Semiconductors by Band Engineering of Highly Directional Electronic States

Daniel I. Bilc[1,2,*], Geoffroy Hautier[3], David Waroquiers[3], Gian-Marco Rignanese[3] & Philippe Ghosez[1,*]
[1] *Theoretical Materials Physics, Université de Liège, 4000 Sart Tilman, Belgium*
[2] *Molecular and Biomolecular Physics Department, National Institute for Research and Development of Isotopic and Molecular Technologies, RO-400293 Cluj-Napoca, Romania*
[3] *Institute of Condensed Matter and Nanosciences, Université catholique de Louvain, 1348 Louvain-la-neuve, Belgium*

Thermoelectrics are promising to address energy issues but their exploitation is still hampered by low efficiencies. So far, much improvement has been achieved by reducing the thermal conductivity but less by maximizing the power factor. The latter imposes apparently conflicting requirements on the band structure: a narrow energy distribution and a low effective mass. Quantum confinement in nanostructures or the introduction of resonant states were suggested as possible solutions to this paradox but with limited success. Here, we propose an original approach to fulfill both requirements in bulk semiconductors. It exploits the highly-directional character of some orbitals to engineer the band-structure and produce a type of low-dimensional transport similar to that targeted in nanostructures, while retaining isotropic properties. Using first-principles calculations, the theoretical concept is demonstrated in Fe_2YZ Heusler compounds, yielding power factors 4-5 times larger than in classical thermoelectrics at room temperature. Our findings are totally generic and rationalize the search of alternative compounds with a similar behavior. Beyond thermoelectricity, these might be relevant also in the context of electronic, superconducting or photovoltaic applications.

PACS numbers: 71.15.-m, 71.15.Mb, 71.20.-b, 71.20.Be, 71.20.Nr, 72.10.-d, 72.20.Pa, 73.21.-b

Thermoelectricity, realizing the direct conversion between thermal and electrical energies, is a very promising avenue for renewable energy generation. The efficiency of a thermoelectric (TE) material can be described by its figure of merit ZT, defined as $ZT=(S^2\sigma T)/(\kappa_e+\kappa_l)$, where S is the thermopower, σ the electrical conductivity, T the absolute temperature, and κ_e and κ_l are the electronic and lattice contributions to the thermal conductivity. In practice, ZT should be greater than 3 for TE devices to become fully competitive with other energy conversion systems [1, 2]. Unfortunately, more than fifty years after the promising discovery of Bi_2Te_3-based alloys with $ZT\sim1$ [3], increasing ZT further remains a real challenge. Huge efforts have been dedicated to the lowering of κ_l using specific crystal structures (e.g., phonon glass-electron crystals [4]) and nanostructuring [5–9], leading to the generation of materials with ZT=1 – 2.4 within the last decade [10–12]. Record low values κ_l=0.22 – 0.5 W/mK [8, 10] were achieved and it is unlikely that these values can still be significantly decreased. At this stage, as emphasized by Kanatzidis [8], the next step forward should come from new breakthrough ideas on how to significantly enhance $S^2\sigma$, the power factor (PF).

A promising avenue was proposed by Hicks and Dresselhaus [5, 13] who predicted theoretically that quantum confinement of electrons in multiple wells can substantially increase the PF. It was confirmed experimentally that the PF in the confined region of nanostructures [14, 15] can indeed be larger than in related bulks. However, the gain in the confined region is partly counterbalanced by the contribution from the barrier material producing the confinement. More recently, Mahan and Sofo [16] searched for what should be the ideal shape of the so-called "transport distribution function" that optimizes ZT. They reached the conclusion that the best materials would combine (i) a distribution of carrier energy as narrow as possible and (ii) high carrier velocities in the direction of the applied field. Satisfying both of these two criteria seems difficult in practice: narrow energy distributions are typically associated with flat energy bands while high carrier velocities are necessarily associated with highly dispersive bands. This could partly be achieved in rare-earth compounds like $YbAl_3$, yielding very large PF at low temperature [17]. However, those are metals with TE properties rapidly decreasing with increasing T. Alternatively, attempts to combine these apparently incompatible requirements in semiconductors have relied on the "band structure engineering" of narrow energy features in the density of states from in-gap and resonant states near the band edges [18–22].

Here, we show theoretically that the seemingly conflicting requirements formulated by Mahan and Sofo [16] can actually be combined within the same band of certain semiconductors, exploiting the highly-directional character of some orbitals. This is achieved without any nanostructuring or introduction of resonant states. It yields, in the bulk phase, a type of low-dimensional transport similar to that targeted by Hicks and Dresselhaus in nanostructures [5], while simultaneously retaining isotropic transport properties at the macroscopic level, concretizing ideas recently proposed by Parker *et al.* [23]. The concrete consequences of this finding on the TE

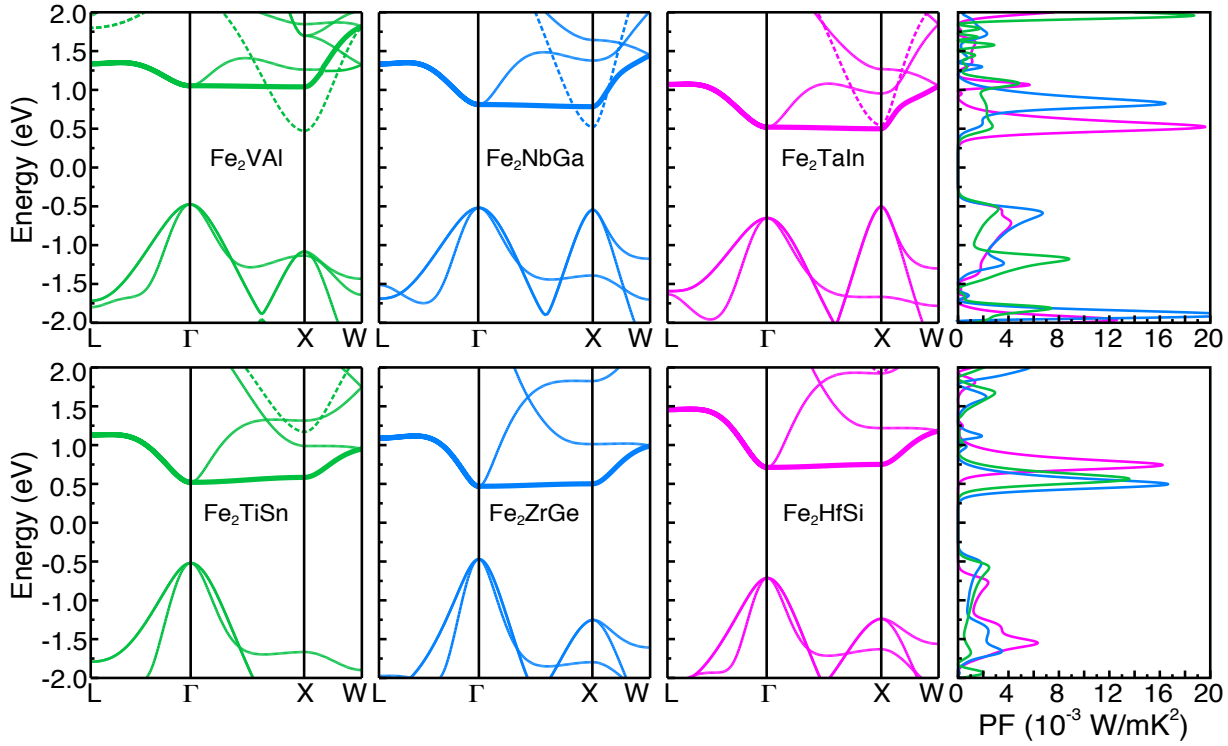

FIG. 1: **Electronic band structures and power factors (PF=$S^2\sigma$) at 300 K for the sets S1 and S2 of compounds.** Fe_2YZ full Heusler compounds with Y=V (green), Nb (blue), Ta (magenta) and Z=Al, Ga, In in 1^{st} row. Fe_2YZ full Heusler compounds with Y=Ti (green), Zr (blue), Hf (magenta), and Z=Sn, Ge, Si in 2^{nd} row. Dotted lines indicate the highly-dispersive lowest conduction band of dominant Y e_g character. The bold lines shows the band of Fe e_g character that is flat along the ΓX direction and highly-dispersive along others.

properties is demonstrated in the class of Fe_2YZ full Heusler compounds: by engineering the appearance of Fe e_g states at the bottom of the conduction bands, power factors 4-5 times larger than in classical thermoelectrics (such as PbTe or Bi_2Te_3) can be obtained at room temperature. Beyond revealing the unexpected interest of a class of compounds often considered as modest thermoelectrics [24], our results rationalize the search of alternative compounds with optimal power factor. The underlying concepts are totally generic and can be combined with other known strategies for decreasing the thermal conductivity in order to increase the TE figure of merit.

The electronic properties were studied within density functional theory using CRYSTAL [25]. We adopted a B1-WC hybrid functional scheme [26], which was previously shown accurate for describing the electronic and TE properties of this class of compounds [21]. The electronic transport properties were studied within the Boltzmann transport formalism and constant relaxation time approximation as implemented in BoltzTraP [27]. Within this approximation S is independent of the relaxation time τ, whereas σ and PF depend linearly on τ. The relaxation time was set to τ=3.4×10^{-14} s in all the calculations. This value was determined by fitting the electrical resistivity ρ to the experimental value of 0.65 mΩcm for $Fe_2VAl_{1-x}M_x$ (M = Si, Ge) systems at doping x=0.03 and 300K [24, 28]. For Fe_2VAl, the calculated PF is 3 mW/mK^2 (Fig. 1) in close agreement with experimental data. In order to estimate with more accuracy ZT at high T, we went beyond constant relaxation time approximation and considered T and energy E dependences of the relaxation time $\tau(T, E)$ for the acoustic and polar optical phonon scattering mechanisms (Ref. [29], text). The thermodynamical stability was assessed using the generalized gradient approximation (GGA) from Perdew Burke and Ernzheroff (PBE) within a plane augmented wave (PAW) approach and using VASP [53, 54]. The computational parameters and pseudopotentials are similar to the ones used in the Materials Project [55, 56]. For each chemical system (e.g., Fe-Ti-Sn), we computed the chemistry in the Heusler crystal structure but also other ternary crystal structures obtained from Heusler-forming systems. The stability of each Heusler phase was evaluated versus all phases present in the Materials Project and our generated ternary phases using the convex hull construction as implemented in the pymatgen package [57].

We start our search from Fe_2VAl that, in spite of rel-

atively modest TE properties (ZT∼0.13-0.2 [24, 58], PF = 4-6 mW/mK^2 [24, 28] at 300-400 K), is considered for low-cost TE applications [59]. As clarified recently [21], it is an intrinsic semiconductor, with a low band gap between the highest valence bands of dominant Fe t_{2g} character and a highly-dispersive lowest conduction band of dominant V e_g character (see dotted line in Fig. 1). Interestingly Fe_2VAl also exhibits a "flat-and-dispersive" band of Fe e_g character that is very flat along the ΓX direction of the Brillouin zone (BZ) and highly dispersive along others (see bold line in Fig. 1). This band combines the above-mentioned features identified by Mahan and Sofo to produce a large PF. It lies however ∼0.6 eV above the bottom of the conduction band, and is not active in transport at room temperature for optimal doping at electron concentrations n∼10^{19} cm^{-3}. In order to move its position towards the bottom of the conduction band we performed atomic substitutions at Y and Z sites.

We consider in Fig. 1 a first set (S1) of Fe_2YZ full Heusler compounds with Y=V, Nb, Ta and Z=Al, Ga, In. Going from 3d to 5d transition metal elements at the Y site tends to move the Y e_g dispersive band upwards. Furthermore, going to higher-mass elements at Y and Z sites increases the lattice parameter (and the Fe-Fe distance), resulting in a decrease of Fe-Fe interactions lowering the Fe e_g levels (Ref. [29], text). Consequently, in many compounds, the Fe e_g flat-and-dispersive band appears close to the bottom of the conduction band. In line with our expectations, this increases the PFs at 300K from ∼3 mW/mK^2 for Fe_2VAl to ∼12 mW/mK^2 for Fe_2NbAl and Fe_2TaAl and up to 16-20 mW/mK^2 for Fe_2NbGa, Fe_2TaGa, Fe_2NbIn and Fe_2TaIn (Fig. 1, and Ref. [29], Fig. 4). Band-by-band analysis for Fe_2TaIn shows that most of the PF (90 %) comes from the Fe e_g flat-and-dispersive band (Ref. [29], Fig. 6).

In a second set (S2) of Fe_2YZ compounds with Y=Ti, Zr, Hf, and Z=Si, Ge, Sn, the dispersive Y e_g band is pushed up even higher in energy. It appears well above the Fe e_g bands, that are now the only lowest conduction bands (Fig. 1, and Ref. [29], Fig. 5). These compounds exhibit also extremely large PFs of ∼14-17 mW/mK^2 at 300K, consistently with what was reported in Ref. [60]. This time, the large PF is almost entirely generated by the Fe e_g flat-and-dispersive band (∼93 % of the total PF for Fe_2TiSn (Ref. [29], Fig. 6).

In all S1 and S2 compounds exhibiting enhanced TE properties, the PF remains substantial (i.e. keeps 90% of its peak value) in a similar and relatively wide range of carrier concentrations ($n \approx 4\times10^{20}$ - 3×10^{21} cm^{-3}) at which $|S|$∼150-200 μV/K. These compounds then exhibit large S, comparable to those of Fe_2VAl and the best classical thermoelectrics, but at n and σ values that are about one order of magnitude larger (Ref. [29], Fig. 7).

Taking Fe_2TiSn as a representative example, the inspection of the carriers contributing to the transport properties at 300K provides further insight into the enhancement of the PFs respect to Fe_2VAl (Fig. 2c and d). In the latter, the sizable TE properties at optimal doping arise from electrons located in small pockets centered at X and associated to highly-dispersive V e_g bands (Fig. 2c). In Fe_2TiSn, the enhanced transport properties at optimal doping are produced instead by electrons from the Fe e_g lowest-conduction states located in three orthogonal tubes extending along $\Gamma - X$ directions and intersecting at Γ (Fig. 2d). These tubes can be viewed as the juxtaposition along the entire $\Gamma - X$ direction of consecutive electron pockets similar to those of Fe_2VAl, so explaining the improved transport properties. This is an optimal realization of the concept of pocket engineering brought forward by Snyder *et al.* [61] where large S and σ values are obtained without compromising mobility by introducing degenerate low effective mass pockets in the Brillouin Zone.

In each cartesian direction, the Heusler Fe_2YZ structure can be seen as made of Fe_2 (alternating with YZ) atomic planes. For clarity, only the family of {001}-Fe_2 planes is illustrated in Fig. 2a but similar families can be drawn along the two other cartesian directions. The tubular shape of the Fermi surface of Fe_2TiSn and related compounds is originating from the highly-directional character of the Fe e_g orbitals. The conduction states of the three tubes in Fig. 2d are associated to the flat band along ΓX (and symmetrically equivalent ΓY and ΓZ directions) in Fig. 1. For the tube along z, these states are made of Fe $d_{x^2-y^2}$ orbitals (see Ref. [29] Fig. 3) which strongly overlap in {001}-Fe_2 planes (strong σ^* bonds along x and y, Fig. 2b) but do not interact significantly from plane to plane (weak δ^* bonds along z). The same is true, *mutatis mutandis*, for the tubes along x and y. This anisotropy of the orbital interactions gives rise to electronic bands that are highly-dispersive in two directions (m_t∼0.3 m_e for Fe_2TiSn and m_t∼0.2 m_e for Fe_2TiSi) and flat in the third one (m_l∼26 m_e for Fe_2TiSn and m_l∼90 m_e for Fe_2TiSi), so concretizing the ideas of Mahan and Sofo [16]. The tubular shape of the Fermi surface comes from the large effective mass ratio (R=m_l/m_t∼87 for Fe_2TiSn and R∼450 for Fe_2TiSi) and highlights that these compounds exhibit a kind of two-dimensional electronic transport in Fe_2 planes [62], similar to what was proposed in nanostructures in order to realise increased TE performance [5]. Here however, it is achieved in bulk cubic compounds. This yields a periodic repetition of two-dimensional conductive channels (i.e. Fe_2 planes) at the ultimate unit-cell scale. Moreover, the isotropic character of the properties is preserved through the coexistence of symmetry equivalent families of {001}-, {010}- and {100}-Fe_2 planes. In practice however, all the conductive electrons are not similarly contributing to

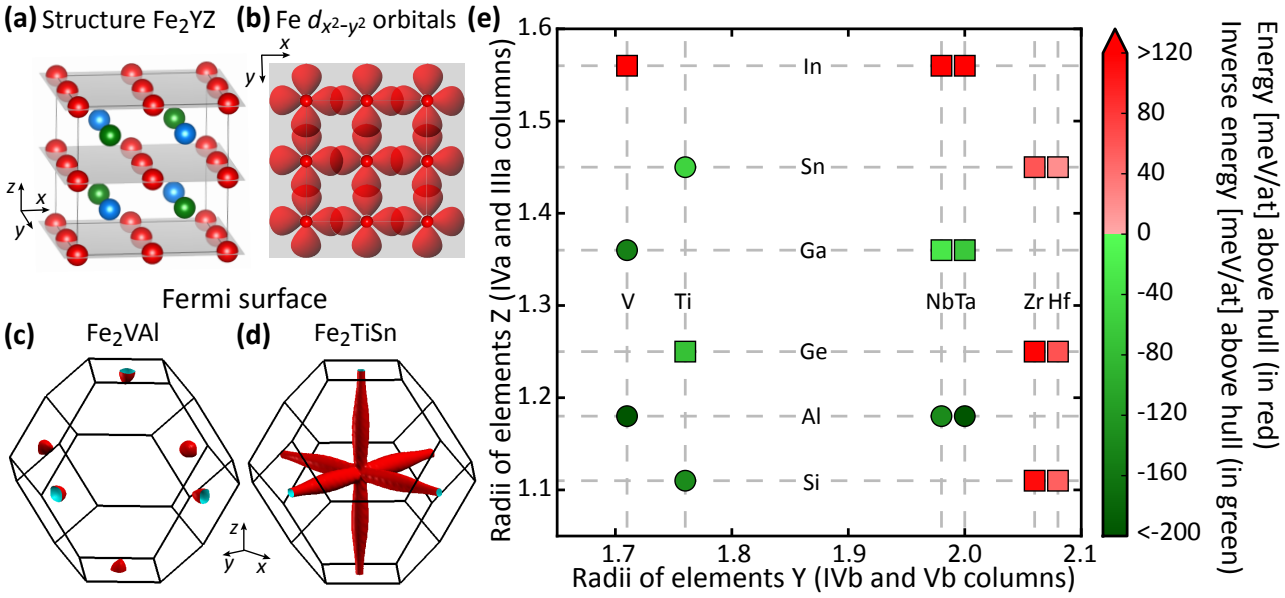

FIG. 2: **Atomic structure, Fermi surfaces, and thermodynamical stability of Fe_2YZ compounds.** **(a)** Full Heusler structure consisting of four interpenetrating fcc lattices with Fe, Y and Z atoms represented in red, green and blue. It can also be viewed as alternating Fe_2 and YZ planes along the {001} (see Fe_2 planes highlighted in grey), {100}, and {010} directions. **(b)** Sketch of the Fe $d_{x^2-y^2}$ e_g orbitals overlapping in {001}-Fe_2 planes. **(c,d)** Fermi surfaces of Fe_2VAl and Fe_2TiSn at doping concentration yielding the maximum PFs at 300K. **(e)** Map of the thermodynamical stability (as measured by the energy with respect to hull) computed at 0 K as a function of the Y and Z atomic radii. A negative number (inverse energy above hull, green color) corresponds to a stable phase and a positive number (energy above hull, red color) to an unstable one. Circles (resp. squares) correspond to compounds (resp. not) previously synthesized.

transport in a given direction: for instance, only the states in the tubes along x and y ({100}- and {010}-Fe_2 planes) contribute significantly to the transport along z. All this is a concrete illustration that low-dimensional electronic structures can occur in high-symmetry cubic systems, as also proposed recently by Parker *et al.* [23] in another class of compounds.

From the practical point of view, a central issue concerns the thermodynamical stability of the S1 and S2 compounds. This was investigated at the first-principles level (Ref. [29], text). The results are summarized in Fig. 2e. Stable and unstable phases are associated respectively with green and red colors. Compounds previously synthesized are stable. Fe_2TiGe and Fe_2NbGa with good TE performance are predicted to be fully stable. We see that including elements like In, Zr or Hf with large ionic radii tend to destabilize the Heusler structure, although the synthesis of Fe_2HfSn might stay experimentally accessible. Another practical issue concerns the appearance of anti-site defects in these Heusler compounds, which are detrimental to the TE performance [21]. From our calculations in Ref. [29] Table 2, S2 compounds appear to be less prone to form anti-site defects than Fe_2VAl.

The existence of several isostructural stable compounds with very attractive PF is an advantage for TE applications. Combining such compounds in solid solutions should allow the reduction of κ_l [9] while preserving the shape of their electronic band structure at the conduction band bottom (nearly identical since dominated by the same Fe e_g states, see Ref. [29] Figure 5) and the related large PF. Such a reduction of κ_l has been demonstrated in $Fe_2V_{1-x}W_xAl$ alloys [58], reaching values of $\sim$3 W/mK. The presence of heavier elements than V and Al is likely to lower κ_l of the new Heusler candidates compared to Fe_2VAl. In this context, reasonably low values can be expected, for instance, in Fe_2TiSn and its solid solutions (e.g., $Fe_2TiSn_{1-x}Si_x$). With κ_l=3.5 W/mK, we estimate ZT values larger than 1 for Fe_2TiSn in the temperature range between 600-900K (Ref. [29], Fig. 10). Such large ZT values are achieved at carrier concentrations only slightly lower than those corresponding to the optimum PF and at which S and n remain large. These ZT values are significantly larger than those predicted for Fe_2VAl, which properly reproduce the experiment (ZT = 0.2 at 400K with κ_l=3.3 W/mK, in agreement with Ref. [58]). This attests that the beneficial effect on the PF, achieved through the low-dimensional transport in Fe_2TiSn, can be accompanied by a significant increase of ZT, without being systematically counter-balanced by another detrimental effect.

The excellent TE properties of some of the Fe_2YZ compounds demonstrated theoretically in this work, combined with the low-cost and wide availability of their constitutive elements, make them very attractive for large-

scale TE applications, well beyond what could have been anticipated from previous studies of Fe_2VAl. Going further, our results also highlight that, contrary to the current belief, extremely large PF can be intrinsic to bulk semiconductors. Our work rationalizes how this can be achieved in practice through the engineering of highly-directional states at the bottom of the conduction bands, yielding low-dimensional transport. This calls for the search of alternative families of compounds realizing the same ideas. The link that we establish with some basic requirements on the electronic band structure is particularly relevant to succeed identifying such compounds in the current context of emergent high-throughput search of alternative thermoelectrics [63, 64] that requires clear and simple design rules. Our findings might also attract interest well beyond the field of thermoelectrics: the singular Fermi surface in these systems present close similarities with those of Fe-based superconductors [65] and the associated low-dimensional transport might be relevant in the context of some electronic [66] or photovoltaic [67] applications.

We thank P. Jacques, J.-P. Issi and N. Bristowe for useful discussions. Work supported by EnergyWall project CoGeTher, ARC project TheMoTherm, FNRS project HiT4FiT, and a collaboration between WBI and the Romanian Academy of Sciences. Ph.G. thanks a Research Professorship of the Francqui Foundation, D.I.B. the Romanian National Authority for Scientific Research, CNCS-UEFISCDI (Grant No. PN-II-RU-TE-2011-3-0085), G. H. and G.-M. R. the F.R.S.-FNRS and G. H. the European Marie Curie CIG (Grant No. HTforTCOs PCIG11-GA-2012-321988). Calculations were performed at Céci HPC Center, funded by F.R.S.-FNRS.*Correspondence should be addressed to D.I.B. (Daniel.Bilc@itim-cj.ro) and Ph.G. (Philippe.Ghosez@ulg.ac.be).

[1] T. M. Tritt and M. A. Subramanian, MRS Bulletin **31**, 188 (2006).
[2] C. J. Vineis, A. Shakouri, A. Majumdar, and M. G. Kanatzidis, Adv. Mater. **22**, 3970 (2010).
[3] H. J. Goldsmid and R. W. Douglas, Brit. J. Appl. Phys. **5**, 386 (1954).
[4] G. A. Slack, in CRC Handbook Of Thermoelectrics, CRC Press, Boca Raton, pp 407-440 (1995).
[5] L. D. Hicks and M. S. Dresselhaus, Phys. Rev. B **47**, 12727 (1993).
[6] G. Chen, M. S. Dresselhaus, G. Dresselhaus, J. P. Fleurial, and T. Caillat, Int. Mater. Rev. **48**, 45 (2003).
[7] J. G. Snyder and E. S. Toberer, Nature Mater. **7**, 105 (2008).
[8] M. G. Kanatzidis, Chem. Mater. **22**, 648 (2010).
[9] K. Biswas *et al.*, Nature **489**, 414 (2012).
[10] R. Venkatasubramanian, E. Siivola, V. Colpitts, and B. O´Quinn, Nature **413**, 597 (2001).
[11] T. C. Harman, P. J. Taylor, M. P. Walsh, and B. E. LaForge, Science **297**, 2229 (2002).
[12] K. F. Hsu *et al.*, Science **303**, 818 (2004).
[13] J. P. Heremans, M. S. Dresselhaus, L. E. Bell, and D. T. Morelli, Nature Nanotech. **8**, 471 (2013).
[14] L. D. Hicks, T. C. Harman, X. Sun, and M. S. Dresselhaus, Phys. Rev. B **53**, R10493 (1996).
[15] H. Ohta *et al.*, Nature Materials **6**, 129 (2007).
[16] G. D. Mahan and J. O. Sofo, Proc. Natl. Acad. Sci. USA **93**, 7436 (1996).
[17] D. M. Rowe, V. L. Kuznetsov, L. A. Kuznetsova, and G. Min, J. Phys. D: Appl. Phys. **35**, 2183 (2002).
[18] D. Bilc *et al.*, Phys. Rev. Lett. **93**, 146403 (2004).
[19] S. Ahmad, K. Hoang, and S. D. Mahanti, Phys. Rev. Lett. **96**, 056403 (2006).
[20] J. P. Heremans *et al.*, Science **321**, 554 (2008).
[21] D. I. Bilc and P. Ghosez, Phys. Rev. B **83**, 205204 (2011).
[22] B. Paul, P. K. Rawat, and P. Banerji, Appl. Phys. Lett. **98**, 262101 (2011).
[23] D. Parker, X. Chen, and D. J. Singh, Phys. Rev. Lett. **110**, 146601 (2013).
[24] Y. Nishino, S. Deguchi, and U. Mizutani, Phys. Rev. B **74**, 115115 (2006).
[25] R. Dovesi *et al.*, Z. Kristallogr. **220**, 571 (2005).
[26] D. I. Bilc *et al.*, Phys. Rev. B **77**, 165107 (2008).
[27] G. K. H. Madsen and D. J. Singh, Comput. Phys. Commun. **175**, 67 (2006).
[28] M. Vasundhara, V. Srinivas, and V. V. Rao, Phys. Rev. B **77**, 224415 (2008).
[29] See Supplemental Material at http://link.aps.org/supplemental/10.1103/PhysRevLett.114.136601, which includes Refs. [30-52], for further technical details and data supporting our results.
[30] I. de P. R. Moreira, R. Dovesi, C. Roetti, V. R. Saunders, R. Orlando, Phys. Rev. B **62**, 7816 (2000).
[31] E. Ruiz, M. Llunell, P. Alemany, J. Solid State Chem. **176**, 400 (2003).
[32] R. Pandey, M. Causa, N. M. Harrison, M. Seel, J. Phys.: Condens. Matter **8**, 3993 (1996).
[33] T. Bredow, P. Heitjans , M. Wilkening, Phys. Rev. B **70**, 115111 (2004).
[34] D. Munoz-Ramo, J. L. Gavartin, A. L. Shluger, Phys. Rev. B **75**, 205336 (2007).
[35] A. R. Porter, M. D. Towler, R. J. Needs, Phys. Rev. B **60**, 13534 (1999).
[36] Z. Wu, R. E. Cohen, Phys. Rev. B **73**, 235116 (2006).
[37] A. D. Becke, J. Chem. Phys. **104**, 1040 (1996).
[38] M. Goffinet, P. Hermet, D. I. Bilc, and Ph. Ghosez, Phys. Rev. B **79**, 014403 (2009).
[39] A. Prikockyte *et al.*, Phys. Rev. B **84**, 214301 (2011).
[40] Ye Feng *et al.*, Phys. Rev. B **63**, 165109 (2001).
[41] S. V. Dordevic *et al.*, Phys. Rev. B **66**, 075122 (2002).
[42] P. Blaha *et al.*, WIEN2K, An Augmented PlaneWave+Local Orbitals Program for Calculating Crystal Properties, Techn. Universitat Wien, Austria, 2001.
[43] D. J. Singh, I. I. Mazin, Phys. Rev. B **57**, 14352 (1998).
[44] C. S. Lue, Y.-K. Kuo, J. Appl. Phys. **96**, 2681 (2004).
[45] A. Popescu, L. M. Woods, J. Martin, and G. S. Nolas, Phys. Rev. B **79**, 205302 (2009).
[46] H. Chen, G. Hautier, G. Ceder, J. Am. Chem. Soc. **134**, 19619 (2012).
[47] G. Hautier *et al.*, Phys. Rev. B **85**, 155208 (2012).
[48] Y. Nishino, M. Kato, S. Asano, K. Soda, M. Hayasaki,

and U. Mizutani, Phys. Rev. Lett. **79**, 1909 (1997).
[49] C. S. Lue *et al.*, J. Phys.: Condens. Matter **13**, 1585 (2001).
[50] C. S. Lue *et al.*, Phys. Rev. B **78**, 165117 (2008).
[51] A. Ślebarski, J. Goraus, Phys. Rev. B **80**, 235121 (2009).
[52] M. Perrier *et al.*, Metall. Mater. Trans. A **43**, 4999 (2012).
[53] G. Kresse and J. Furthmüller, Comput. Mat. Sci. **6**, 15 (1996).
[54] J. Perdew, K. Burke, and M. Ernzerhof, Phys. Rev. Lett. **77**, 3865 (1996).
[55] Materials Project, http://www.materialsproject.org
[56] A. Jain *et al.*, Comput. Mater. Sci. **50**, 2295 (2011).
[57] S. P. Ong *et al.*, Comput. Mater. Sci. **68**, 314 (2013).
[58] M. Mikami, Y. Kinemuchi, K. Ozaki, Y. Terazawa, and T. Takeuch, J. Appl. Phys. **111**, 093710 (2012).
[59] M. Mikami, K. Kobayashi, T. Kawada, K. Kubo, and N. Uchiyama, J. Electron. Mater. **38**, 1121 (2009).
[60] S. Yabuuchi, M. Okamoto, A. Nishide, Y. Kurosaki, and J. Hayakawa, Appl. Phys. Express **6**, 025504 (2013).
[61] Y. Pei, X. Shi, A. Lalonde, H. Wang, L. Chen, and G. J. Snyder, Nature **473**, 66 (2011).
[62] The 1D-shape of Fermi surface is associated to 2D transport in real space. Due to the orientation of $d_{x^2-y^2}$ orbitals, the latter can be viewed as the combination of two orthogonal transport channels along the Fe-Fe bonds.
[63] S. Wang, Z. Wang, W. Setyawan, N. Mingo, and S. Curtarolo, Phys. Rev. X **1**, 021012 (2011).
[64] I. Opahle, G. K. H. Madsen, and R. Drautz, Phys. Chem. Chem. Phys. **14**, 16197 (2012).
[65] D. J. Singh, Sci. Technol. Adv. Mater. **13**, 054304 (2012).
[66] Y. Z. Chen *et al.*, Nature Comm. **4**, 1371 (2013).
[67] A. Tebano, E. Fabbri, D. Pergolesi, G. Balestrino, and E. Traversa, ACS Nano **6**, 1278 (2012).